Swansea University
Prifysgol Abertawe

# Lattice studies of Sp(2N) gauge theories using GRID

40th International Symposium on Lattice Field Theory

Niccolò Forzano

3rd August 2023

Collaborators:
Ed Bennett, Peter Boyle, Luigi Del Debbio, Deog Ki Hong, Jong-Wan Lee, Julian Lenz, C.-J. David Lin, Biagio Lucini, Alessandro Lupo, Maurizio Piai, Davide Vadacchino

# Overview

- Framework used: GRID[1] library, running on GPUs.
- Targeted theories: Sp(2N) gauge theories with $N_f$ fundamental fermions, $N_{as}$ 2-antisymmetric fermions. Case study will be Sp(4) with $N_f = 0$, $N_{as} = 4$.
  Plots will refer to this theory, unless stated.
- Lattice used: $\tilde{V}/a^4 = 8^4$ lattice, unless stated.
- Update algorithm used: hybrid Monte-Carlo and rational hybrid Monte-Carlo.
- Algorithm tests:
  - Behaviour of integrators and checks on molecular dynamics details.
  - Tests of implementation of symmetries and fermionic operators.
- Other tests:
  - Parameter scans of Sp(4) theories.
  - Scale setting and topology.
- Based on the work presented in arXiv:2306.11649.



[1] P. Boyle, A. Yamaguchi, G. Cossu and A. Portelli, “Grid: A next generation data parallel C++ QCD library,”[arXiv:1512.03487 [hep-lat]]

# Gauge theories with symplectic group

- The Sp(2N) group is the subgroup of SU(2N) such that $U \Omega U^T = \Omega$ where $\Omega = \begin{pmatrix} 0 & \mathbb{1}_N \\ -\mathbb{1}_N & 0 \end{pmatrix}$

- The lattice (Euclidean) Sp(2N) field theories with $N_f$ and $N_{as}$ fermions have action:

$$S \equiv S_g + S_f$$

$$S_g \equiv \beta \sum_x \sum_{\mu<\nu} \left(1 - \frac{1}{2N} \mathrm{Re}\,\mathrm{Tr}\,\mathcal{P}_{\mu\nu}(x)\right)$$

$$S_f \equiv a^4 \sum_{j=1}^{N_{\mathrm{f}}} \sum_x \overline{Q}^j(x) D_m^{(\mathrm{f})} Q^j(x) + a^4 \sum_{j=1}^{N_{\mathrm{as}}} \sum_x \overline{\Psi}^j(x) D_m^{(\mathrm{as})} \Psi^j(x)$$

# GRID: basic tests of the algorithm

- By measuring the difference in Hamiltonian, $\Delta H$ , evaluated before and after the molecular dynamics evolution (*Creutz equality*)[2]

$$\left\langle \exp\left(-\Delta H\right)\right\rangle = 1$$

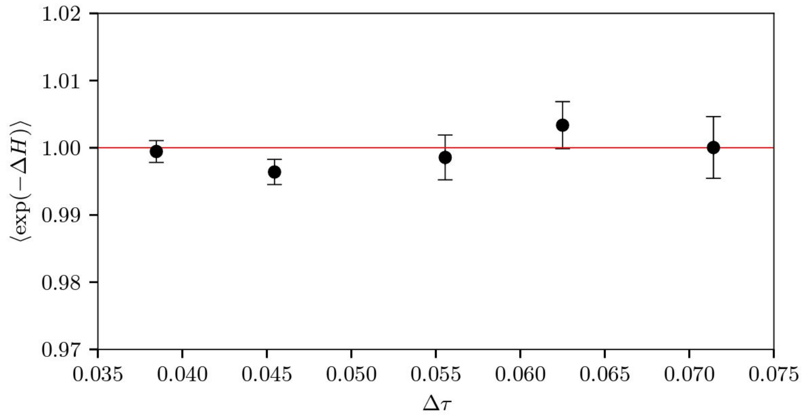


Fig 1: Test of Creutz equality,
$\beta = 6.8$, $am^{as}_0 = -0.6$.

- The ensemble average of the plaquette is independent of the molecular dynamics time-step $\Delta\tau$.

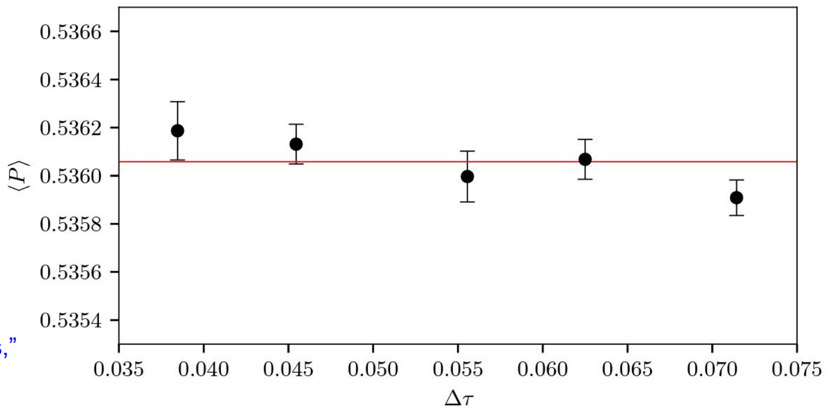


Fig 2: Test of independence of the plaquette on the MD time-step,
$\beta = 6.8$,
$am^{as}_0 = -0.6$.


[2] M. Creutz, “Global Monte Carlo algorithms for many-fermion systems,” Phys. Rev. D 38, 1228-1238 (1988) doi:10.1103/PhysRevD.38.1228

# GRID: basic tests of the algorithm (2)

- Dependence of $\langle \Delta H \rangle$ on $\Delta\tau$, which for a second-order integrator has to scale as

$$\langle \Delta H \rangle \propto (\Delta\tau)^4$$

The best-fit curve is

$$\log\langle \Delta H \rangle = \mathcal{K}_1 \log(\Delta\tau) + \mathcal{K}_2$$

$$\mathcal{K}_1 = 3.6(4) \qquad \chi^2/N_{\mathrm{d.o.f.}} = 0.6$$

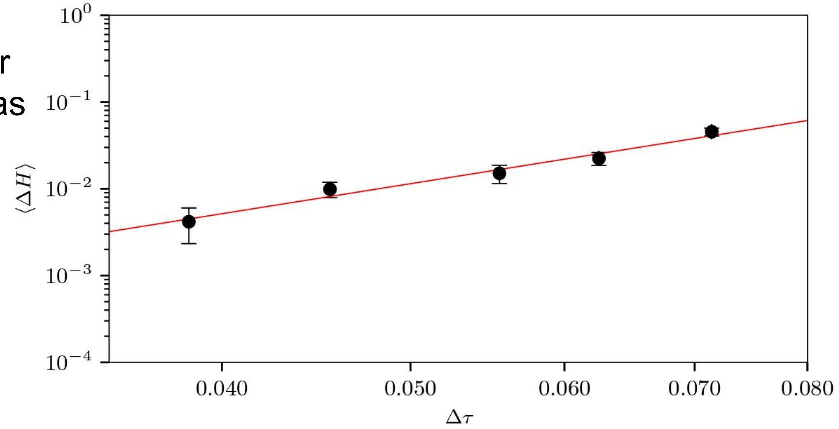


Fig 3: Test of quartic dependence, β = 6.8, $am^{as}_0$ = -0.6.

- We have also tested the expected relation[3] between the acceptance probability and $\langle \Delta H \rangle$

$$P_{\mathrm{acc}} = \mathrm{erfc}\left(\frac{1}{2}\sqrt{\langle \Delta H \rangle}\right)$$

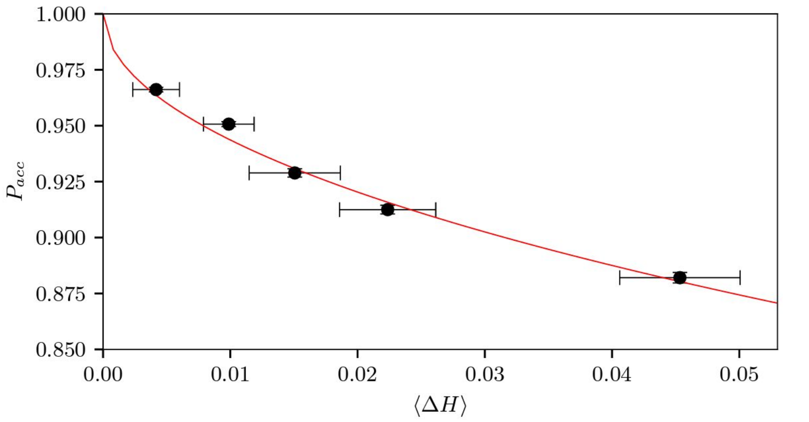


Fig 4: Test of acceptance probability, β = 6.8, $am^{as}_0$ = -0.6.


[3] S. Gupta, A. Irback, F. Karsch and B. Petersson, “The Acceptance Probability in the Hybrid Monte Carlo Method,” Phys. Lett. B 242, 437-443

# GRID: field contribution to the MD force

- Force is splitted in its contribution from the gauge and fermion dynamics[4]

$$F(x,\,\mu) = F_g(x,\,\mu) + F_f(x,\,\mu)$$

- For positive and very large Wilson bare masses, (approaching *quenched regime),* the fermion contribution disappears.

- Conversely, in the opposite regime (*chiral limit*) the fermion contribution become progressively larger.

Approaching chiral limit

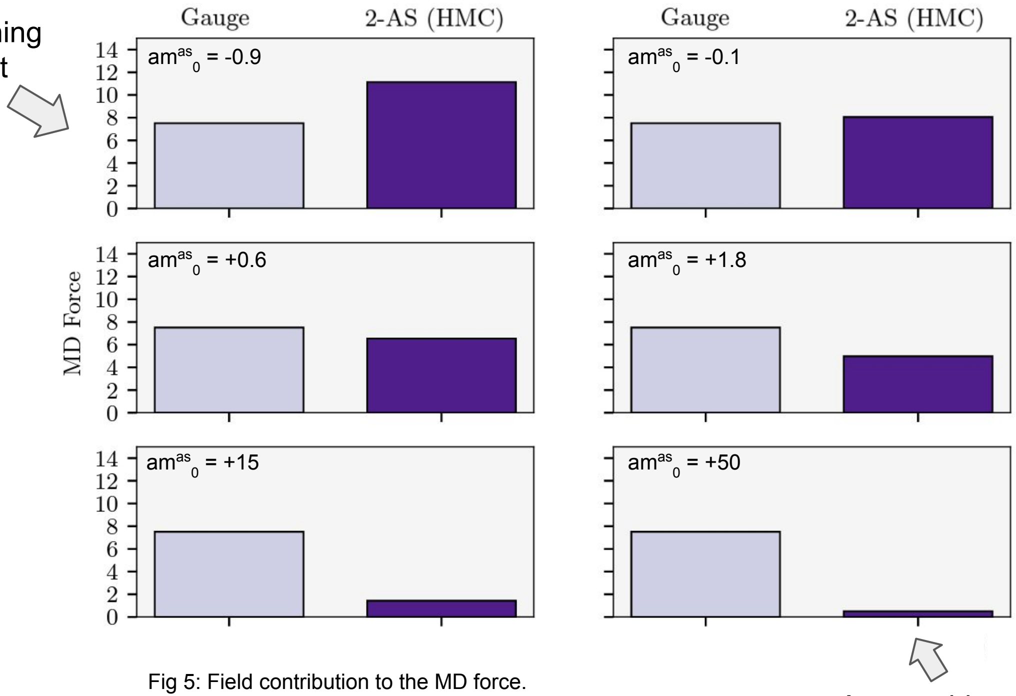


Fig 5: Field contribution to the MD force.

Approaching quenched approximation

[4] L. Del Debbio, A. Patella and C. Pica, “Higher representations on the lattice: Numerical simulations. SU(2) with adjoint fermions,” Phys. Rev. D 81

# The N = 2 quenched theory: Distribution of unfolded density of spacing

- Ensemble of gauge configurations without dynamical fermions (*quenched approximation*) can be used to verify that the Dirac fermions are correctly implemented.
- Because the spectrum captures the properties of the theory, the distribution P(s) differs, depending on the symmetry-breaking pattern predicted.
- We compare the results to the exact predictions of *chiral Random Matrix Theory* (chRMT).[5]

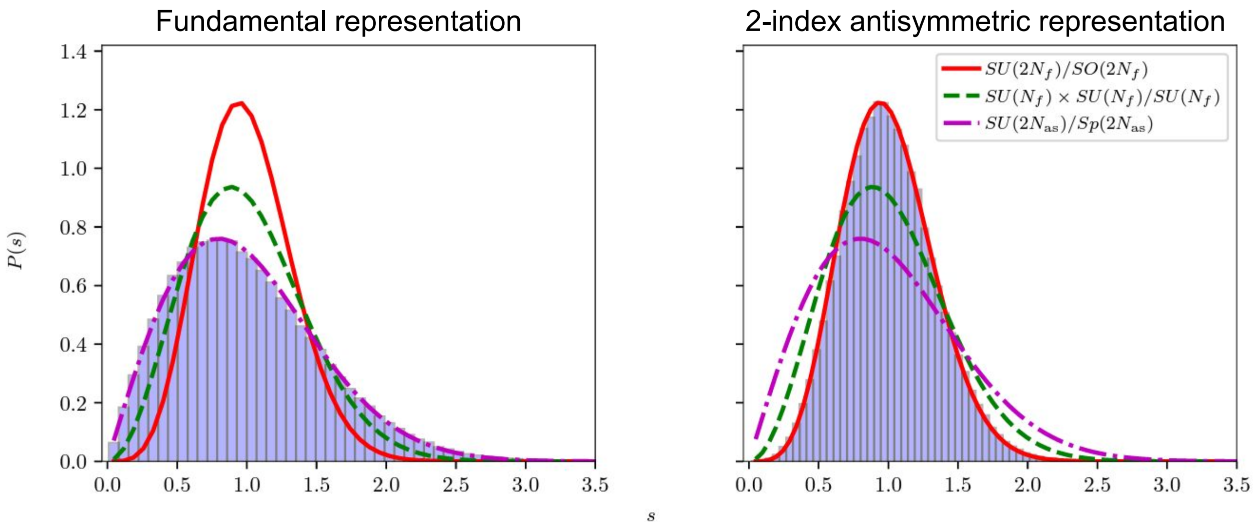


Fig 6: Distribution of the unfolded density of spacing between subsequent eigenvalues of the hermitian Dirac-Wilson operator, $Q_m = \gamma_5 D_m$ where β = 8.0, $am^{as}_0$ = -0.2 , $\tilde{V} = (4a)^4$ .

[5] J. J. M. Verbaarschot, “The Spectrum of the QCD Dirac operator and chiral random matrix theory: The Threefold way,” Phys. Rev. Lett. 72, 2531-2533 (1994) doi:10.1103/PhysRevLett.72.2531 [arXiv:hep-th/9401059 [hep-th]].

# The N = 2 theories coupled to fermions. Bulk phase structure. $N_{as}$ = 4, $N_f$ = 0.

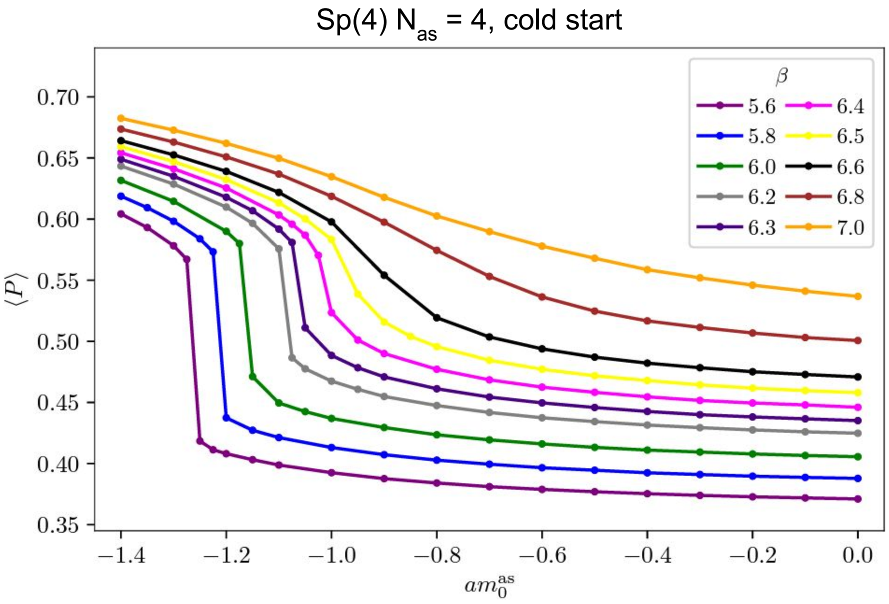


Fig 7: Parameter scan of the Sp(4) theory with $N_{as}$ = 4, $N_f$ = 0 fermions.

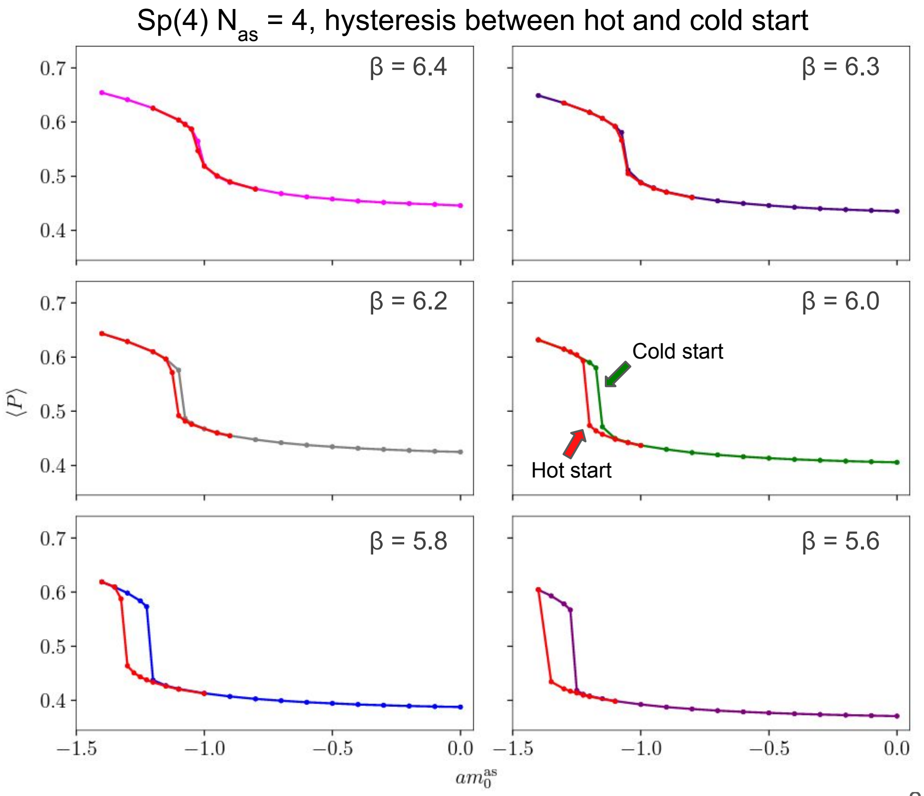


Fig 8: The colour scheme is the same as the figure on the left of the slide.

# Scale setting and topology: Wilson flow

- In the continuum theory, introducing the fifth component, flow time, we solve

$$\frac{\mathrm{d}B_\mu(x,\,t)}{\mathrm{d}t} \;=\; D_\nu G_{\nu\mu}(x,\,t)$$

with boundary conditions

$$B_\mu(x,\,0) = A_\mu(x)$$

- To define a scale, one defines

$$\mathcal{E}(t) \;\equiv\; \frac{t^2}{2}\,\langle \mathrm{Tr}\,[G_{\mu\nu}(t)G_{\mu\nu}(t)]\rangle$$

$$\mathcal{W}(t) \;\equiv\; t\frac{d}{dt}\mathcal{E}(t)$$

and the scales

$$\mathcal{E}(t)|_{t=t_0} = \mathcal{E}_0 \qquad \mathcal{W}(t)|_{t=w_0^2} = \mathcal{W}_0$$

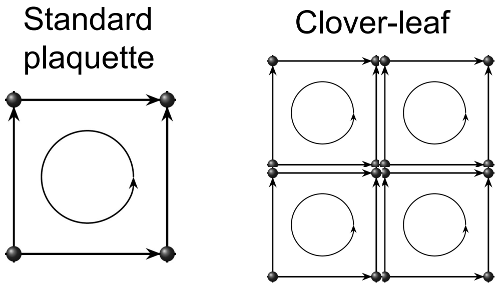


Fig 9: Standard plaquette (left panel) and Clover-leaf Plaquette (right panel), both used for computing Wilson flow.

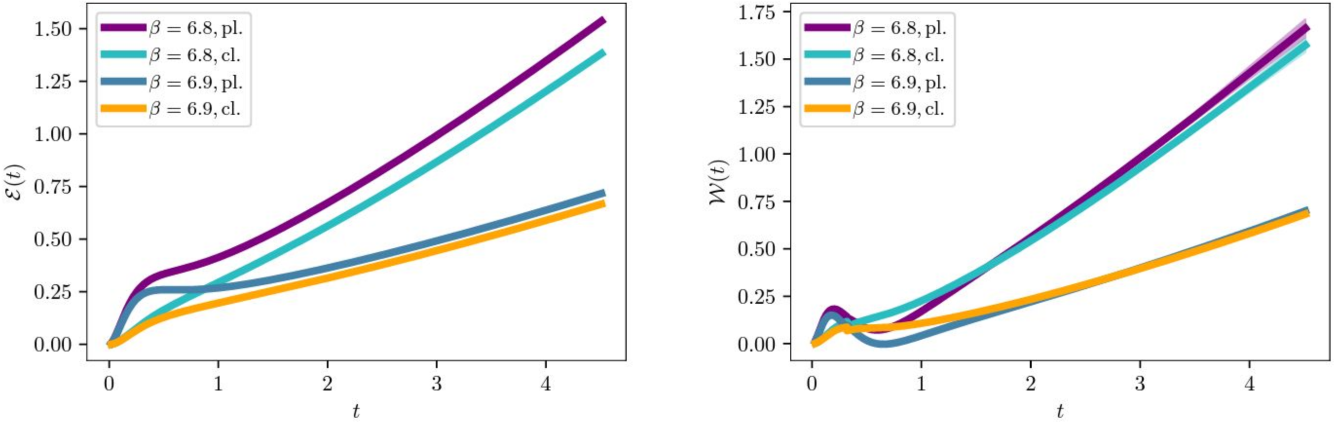


Fig 10: Wilson flow energy density E(t) and W(t), computed from the standard plaquette and the clover-leaf plaquette. $am^{as}_0$ = -0.8 and $\tilde{V} = (12a)^4$ .

# Scale setting and topology: topological charge

- We monitored the evolution of the topological charge,

$$q_L(x,t) \equiv \frac{1}{32\pi^2}\varepsilon^{\mu\nu\rho\sigma}\mathrm{Tr}\left[\mathcal{C}_{\mu\nu}(x,t)\mathcal{C}_{\rho\sigma}(x,t)\right]$$

$$Q_L(t) \equiv \sum_x q_L(x,t)$$

  to show that *topological freezing* was avoided.

- Fit of the histograms are compatible with Gaussian distributions centered at $\langle Q_L(t = w_0^2)\rangle = 0$

- Madras-Sokal[6] integrated autocorrelation time $\tau_Q$ is many orders of magnitude smaller than the number of trajectories.

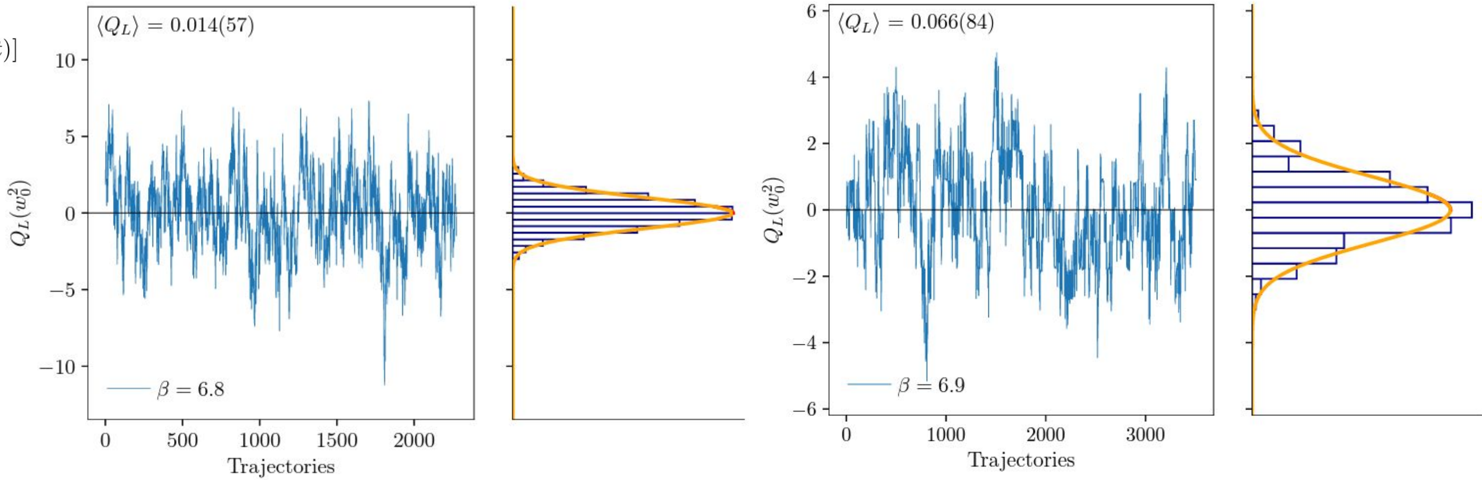


Fig 11: Evolution with the ensemble trajectories of the topological charge, computed at flow time $t = w_0^2$. The lattice size is $\tilde{V} = (12a)^4$ and bare mass $am^{as}_0 = -0.8$.


[6] N.Madras and A.D.Sokal,“The Pivot algorithm:a highly efficient Monte Carlo method for self avoiding walk,”J.Statist. Phys .50 ,109-186 (1988) doi:10.1007/BF01022990

# Summary

- We developed and tested new software, embedded into the GRID environment to take full advantage of its flexibility.
- We reported the (positive) results of our tests of the algorithms.
- We focused particularly on the Sp(4) theory coupled to $N_{as}$= 4 (Dirac) fermions transforming in the antisymmetric representation.
- There are no obvious problems in the software implementation.

# Summary (2)

- This work, and the software we developed for it, set the stage needed to explore and quantify future large-scale studies (e.g. extent of the conformal window).
- The tools we developed can be used also in the context of the recent literature discussing the spectroscopy of Sp(2N) theories with various representations.
- This effort can be complemented and further extended by applying new techniques based on the spectral densities.

Thanks for listening.

# Backup slides

# Sp(2N): Group-theoretical definitions

- The dimension of the group is $$\dim Sp(2N) = (2N+1)N$$

- This implies the block structure $$U = \begin{pmatrix} A & B \\ -B^* & A^* \end{pmatrix}$$

  where the block matrices satisfy $$AB^T = BA^T\ , \qquad AA^\dagger + BB^\dagger = \mathbb{1}_N$$

# More group-theoretical definitions

Expanding the group element U in terms of the hermitian generators $U = \exp(i\omega^a t^a)$

We arrive at the following condition $T\Omega = -\Omega T^*$ where $T = \sum_a \omega^a t^a$.

which implies

$$T = \begin{pmatrix} X & Y \\ Y^* & -X^* \end{pmatrix}$$

where hermiticity imposes the conditions $X = X^\dagger \quad Y = Y^T$

# HMC and RHMC

- Bosonic degrees of freedom $\phi$ and $\phi^\dagger$, known as *pseudofermions*, are introduced replacing a generic number $n_f$ of fermions.

$$(\det D_m^R)^{n_f} = (\det Q_m^R)^{n_f} = \int \mathcal{D}\phi\mathcal{D}\phi^\dagger e^{-a^4 \sum_x \phi^\dagger(x)(Q_m^2)^{-n_f/2}\phi(x)}$$

- A fictitious classical system is defined, described by gauge links and the conjugate momenta $\pi(x,\,\mu) = \pi^a(x,\,\mu)\,t^a$ And the fictitious Hamiltonian is

$$H = \frac{1}{2}\sum_{x,\mu,a} \pi^a(x,\,\mu)\pi^a(x,\,\mu) + H_g + H_f \qquad H_g = S_g \qquad H_f = S_f$$

and the molecular dynamics evolution in fictitious time is dictated by $\frac{\mathrm{d}U_\mu(x)}{\mathrm{d}\tau} = \pi(x,\,\mu)U_\mu(x)\;, \quad \frac{\mathrm{d}\pi(x,\,\mu)}{\mathrm{d}\tau} = F(x,\mu)$ (1)

- The update process can be described as follows:
  - Generate pseudofermions with distribution $e^{-a^4 \sum_x \phi^\dagger(x)(Q_m^2)^{-n_f/2}\phi(x)}$
  - Starting with Gaussian random conjugate momenta, integrating (1) numerically.
  - Accepting or rejecting the gauge configuration by a Metropolis test.

# More details about the lattice theory

The massive Wilson-Dirac operators in the Lagrangian considered are:

$$
\begin{aligned}
D_m^{(\mathrm{f})} Q^j(x) \;\equiv\; & (4/a + m_0^{\mathrm{f}}) Q^j(x) \\
& - \frac{1}{2a} \sum_\mu \Big\{ (1-\gamma_\mu) U_\mu^{(\mathrm{f})}(x) Q^j(x+\hat{\mu}) + (1+\gamma_\mu) U_\mu^{(\mathrm{f}),\dagger}(x-\hat{\mu}) Q^j(x-\hat{\mu}) \Big\}
\end{aligned}
$$

and

$$
\begin{aligned}
D_m^{(\mathrm{as})} \Psi^j(x) \;\equiv\; & (4/a + m_0^{\mathrm{as}}) \Psi^j(x) \\
& - \frac{1}{2a} \sum_\mu \Big\{ (1-\gamma_\mu) U_\mu^{(\mathrm{as})}(x) \Psi^j(x+\hat{\mu}) + (1+\gamma_\mu) U_\mu^{(\mathrm{as}),\dagger}(x-\hat{\mu}) \Psi^j(x-\hat{\mu}) \Big\}
\end{aligned}
$$

# Sp(2N) antisymmetric representation

The link variables in the 2-antisymmetric representation are defined as

$$U^{(\mathrm{as})}_{\mu,\,(ab)(cd)} = \mathrm{Tr}\left(e^{(ab)\,T} U^{(\mathrm{f})}_{\mu} e^{(cd)} U^{(\mathrm{f})\,\mathrm{T}}_{\mu}\right)$$

where $e^{(ab)}$ are an orthonormal basis in the N(2N - 1) - 1 dimensional space of 2N x 2N antisymmetric and $\Omega$ -traceless matrices. The multi-indices $(ab)$ run over $1 \leq a < b \leq 2N$ .
The entry of the basis is defined as follows:

for $b \neq N + a$ we have $$e^{(ab)}_{ij} \equiv \frac{1}{\sqrt{2}}\left(\delta_{aj}\delta_{bi} - \delta_{ai}\delta_{bj}\right)$$

while for $b = N + a$ and $2 \leq a \leq N$ $$e^{(ab)}_{i,i+N} = -e^{(ab)}_{i+N,i} \equiv \begin{cases} \frac{1}{\sqrt{2a(a-1)}}\,, & \text{for } i < a\,, \\ \frac{1-a}{\sqrt{2a(a-1)}}\,, & \text{for } i = a\,. \end{cases}$$

- Transformation of fundamental and 2AS fermions: $Q \to UQ\,, \quad \text{and} \quad \Psi \to U\Psi U^{\mathrm{T}}$

# GRID: basic tests of the algorithm (3)

- Average difference of Hamiltonian evaluated by evolving molecular dynamics forward and backward and flipping the momentum at unitary MD-time.

- Since the Hamiltonian is $\sim 10^6$ and the typical $\delta H \sim 10^{-11}$ violation of reversibility is consistent with relative precision for double-precision floating-point numbers.

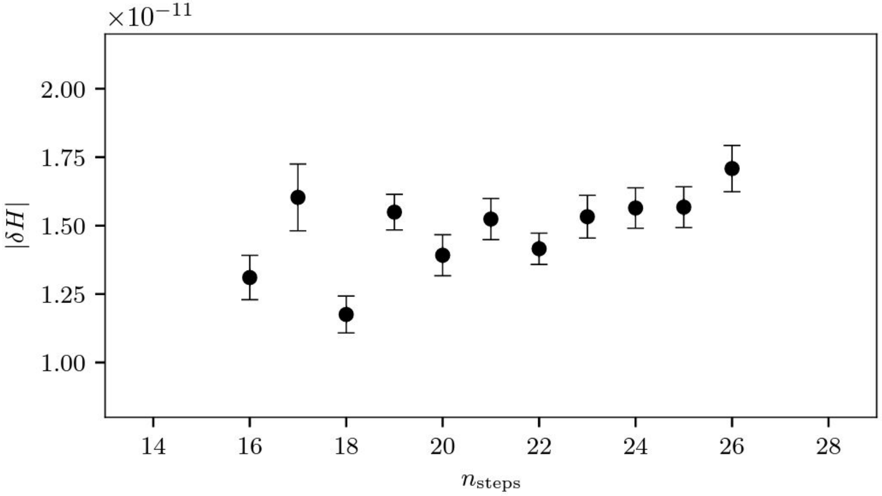


(where $\Delta\tau = \tau/n_{\text{steps}}$)

Fig A: Test of reversibility, β = 6.8, $am^{as}_0$ = -0.6.

# Generators of the algebra in GRID

In GRID, the explicit representation for Sp(4) generators is

$$t_{\mathrm{f}}^{1} = \frac{1}{2\sqrt{2}}\begin{pmatrix} 0 & 1 & 0 & 0 \\ 1 & 0 & 0 & 0 \\ 0 & 0 & 0 & -1 \\ 0 & 0 & -1 & 0 \end{pmatrix} \qquad t_{\mathrm{f}}^{6} = \frac{1}{2}\begin{pmatrix} 0 & 0 & 0 & 0 \\ 0 & 0 & 0 & 1 \\ 0 & 0 & 0 & 0 \\ 0 & 1 & 0 & 0 \end{pmatrix}$$

$$t_{\mathrm{f}}^{2} = \frac{1}{2\sqrt{2}}\begin{pmatrix} 0 & i & 0 & 0 \\ -i & 0 & 0 & 0 \\ 0 & 0 & 0 & i \\ 0 & 0 & -i & 0 \end{pmatrix} \qquad t_{\mathrm{f}}^{7} = \frac{1}{2}\begin{pmatrix} 0 & 0 & i & 0 \\ 0 & 0 & 0 & 0 \\ -i & 0 & 0 & 0 \\ 0 & 0 & 0 & 0 \end{pmatrix}$$

$$t_{\mathrm{f}}^{3} = \frac{1}{2\sqrt{2}}\begin{pmatrix} 0 & 0 & 0 & 1 \\ 0 & 0 & 1 & 0 \\ 0 & 1 & 0 & 0 \\ 1 & 0 & 0 & 0 \end{pmatrix} \qquad t_{\mathrm{f}}^{8} = \frac{1}{2}\begin{pmatrix} 0 & 0 & 0 & 0 \\ 0 & 0 & 0 & i \\ 0 & 0 & 0 & 0 \\ 0 & -i & 0 & 0 \end{pmatrix}$$

$$t_{\mathrm{f}}^{4} = \frac{1}{2\sqrt{2}}\begin{pmatrix} 0 & 0 & 0 & i \\ 0 & 0 & i & 0 \\ 0 & -i & 0 & 0 \\ -i & 0 & 0 & 0 \end{pmatrix} \qquad t_{\mathrm{f}}^{9} = \frac{1}{2}\begin{pmatrix} 1 & 0 & 0 & 0 \\ 0 & 0 & 0 & 0 \\ 0 & 0 & -1 & 0 \\ 0 & 0 & 0 & 0 \end{pmatrix}$$

$$t_{\mathrm{f}}^{5} = \frac{1}{2}\begin{pmatrix} 0 & 0 & 1 & 0 \\ 0 & 0 & 0 & 0 \\ 1 & 0 & 0 & 0 \\ 0 & 0 & 0 & 0 \end{pmatrix} \qquad t_{\mathrm{f}}^{10} = \frac{1}{2}\begin{pmatrix} 0 & 0 & 0 & 0 \\ 0 & 1 & 0 & 0 \\ 0 & 0 & 0 & 0 \\ 0 & 0 & 0 & -1 \end{pmatrix} .$$

# The N = 2 lattice Yang-Mills theory: Polyakov loops

- Considering the pure gauge Sp(4) theory, we verify that centre symmetry, $(\mathbb{Z}_2)^4$ is broken at small volumes, but restored at large volumes, by looking at the *Polyakov loop*

$$\Phi \equiv \frac{1}{N_c N_s^3} \sum_{\vec{x}} \mathrm{Tr} \left( \prod_{t=0}^{t=N_t-1} U_0(t,\vec{x}) \right)$$

- Zero-temperature Sp(4) lattice theory expected to preserve the centre symmetry (*confinement*): verified for sufficiently large volumes.

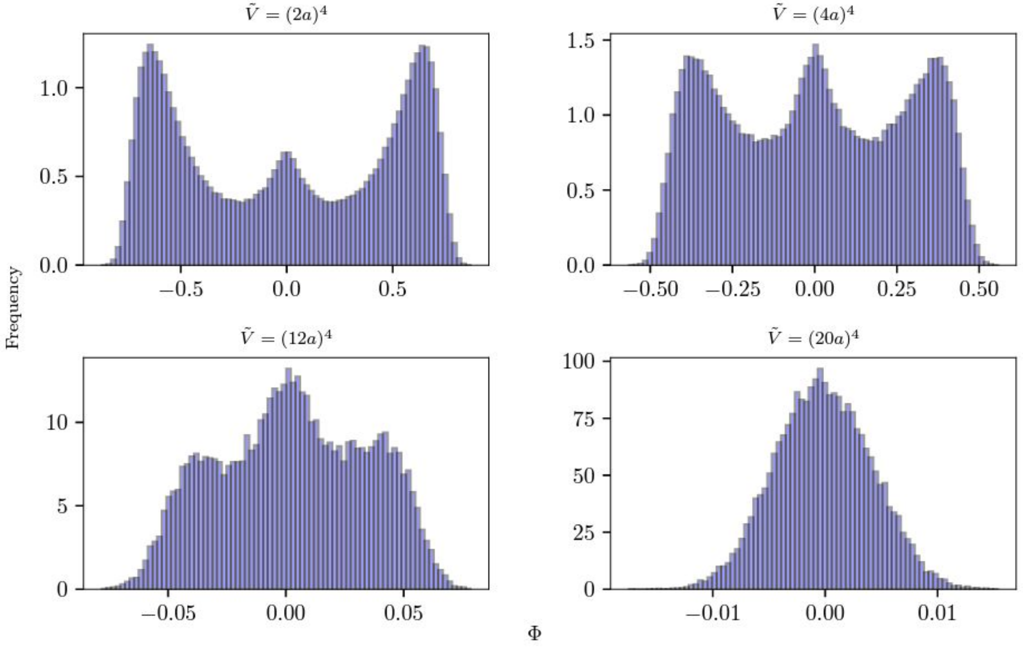


Fig B: Study of finite-size effects on the lattice, for the Sp(4) Yang-Mills theory, β = 9.0 and $\tilde{V} = (2a)^4, (4a)^4, (12a)^4, (20a)^4$ .

# GRID: comparing HMC and RHMC

- As we will consider also odd numbers of fermions, we compute the average plaquette

$$P \equiv \frac{a^4}{6\tilde{V}} \sum_x \sum_{\mu<\nu} \left[ \frac{1}{2N} \mathrm{Re}\,\mathrm{Tr}\,\mathcal{P}_{\mu\nu}(x) \right]$$

  for:

  - All fermions with the HMC
  - Two fermions with HMC and two with RHMC
  - All fermions with RHMC.

- No visible discrepancies are detected.

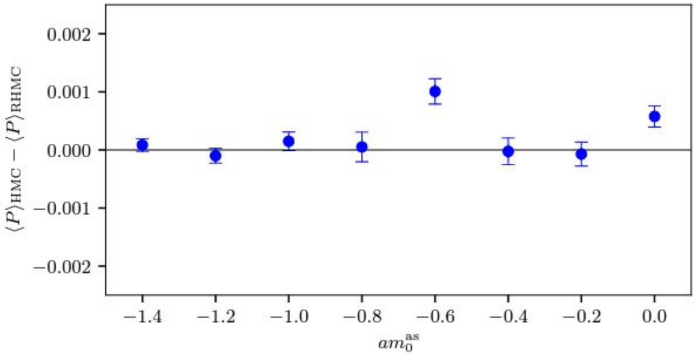


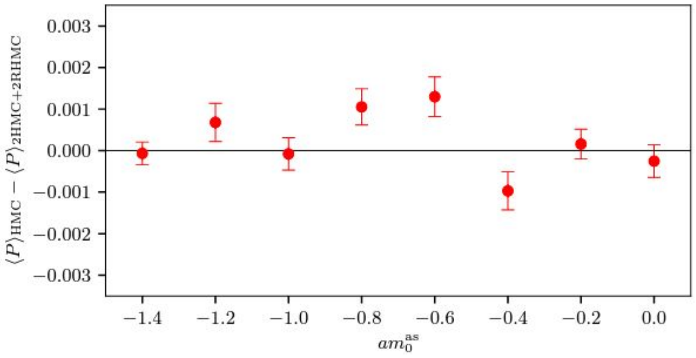


Fig C: Compatibility between plaquette averages obtained with HMC and RHMC algorithms for the theory N = 2, $N_f$ = 0, $N_{as}$ = 4, β = 6.8, -1.4 ≤ $am^{as}_0$ ≤ 0.0

# Deconfinement with Polyakov loops

- The expectation value of a Polyakov loop[7] determines the free energy $F_q$ of a static quark as a function of the inverse temperature 1/T according to

$$\langle\phi(\vec{n})\rangle = \exp\left(-\frac{F_q}{T}\right)$$

and the correlation function of two Polyakov loops yields the static quark-antiquark free energy $F_{q\bar{q}}$

$$\langle\phi(\vec{n})\phi^{\dagger}(\vec{m})\rangle = \exp\left(-(\vec{n}-\vec{m})\,\frac{F_{q\bar{q}}}{T}\right)$$

Therefore, static quarks will be confined if this correlation function vanishes when $|\vec{n}-\vec{m}| \to 0$ .

[7] A. M. Polyakov, Phys. Lett. B 72 (1978), 477-480 doi:10.1016/0370-2693(78) 90737-2

# chRMT, Distribution of folded density of spacing

- According to ref. [5] , the folded density of spacing

$$P(s) = N_{\tilde{\beta}} s^{\tilde{\beta}} \exp\left(-c_{\tilde{\beta}} s^2\right) , \quad \text{where} \quad N_{\tilde{\beta}} = 2\frac{\Gamma^{\tilde{\beta}+1}\left(\frac{\tilde{\beta}}{2}+1\right)}{\Gamma^{\tilde{\beta}+2}\left(\frac{\tilde{\beta}+1}{2}\right)}, \; c_{\tilde{\beta}} = \frac{\Gamma^2\left(\frac{\tilde{\beta}}{2}+1\right)}{\Gamma^2\left(\frac{\tilde{\beta}+1}{2}\right)}$$

$$s = \frac{n_{i+1}^{(c)} - n_i^{(c)}}{\mathcal{N}}$$

$$c = 1, \cdots, N_{\text{conf}}$$

- The Dyson index $\tilde{\beta}$ can take three different values:

For $\tilde{\beta} = 1$ , we will have $SU(2N_f) \to Sp(2N_f)$

For $\tilde{\beta} = 2$ , we will have $SU(N_f) \times SU(N_f) \to SU(N_f)$

For $\tilde{\beta} = 4$ , we will have $SU(2N_f) \to SO(2N_f)$

# Madras-Sokal windowing algorithm

- According to Madras-Sokal widowing algorithm, the integrated autocorrelation time of a finite sample $A_1$, …, $A_n$ is

$$\hat{\tau}_{\text{int}} \equiv \frac{1}{2} \sum_{t=-(n-1)}^{n-1} \lambda(t)\, \hat{\rho}(t) \qquad\qquad \operatorname{var}(\hat{\tau}_{\text{int}}) \approx \frac{2(2M+1)}{n} \tau_{\text{int}}^2$$

and $\hat{\hat{\rho}}(t) \equiv \hat{\hat{C}}(t)/\hat{\hat{C}}(0)$ $\quad \hat{\hat{C}}(t) \equiv \frac{1}{n-|t|} \sum_{i=1}^{n-|t|} (A_i - \bar{A})(A_{i+|t|} - \bar{A})$ $\quad \lambda(t) = \begin{cases} 1 & \text{if} \quad |t| \leqslant M \\ 0 & \text{if} \quad |t| > M \end{cases}$

where M is a suitable chose cut-off.

# Standard plaquette and Clover-leaf plaquette

- Standard plaquette:

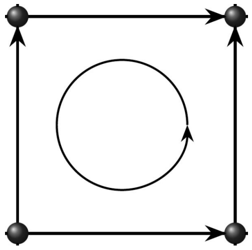

$$\mathcal{P}_{\mu\nu}(x) \equiv U_\mu(x)U_\nu(x+\hat{\mu})U_\mu^\dagger(x+\hat{\nu})U_\nu^\dagger(x)$$

- Clover-leaf plaquette:

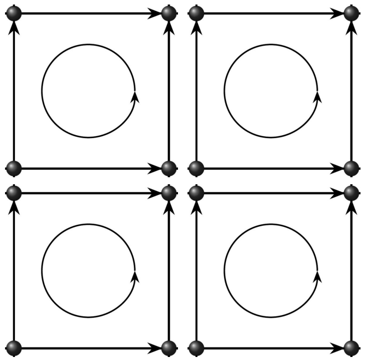

$$\begin{aligned}\mathcal{C}_{\mu\nu}(x) \;\equiv\; \frac{1}{8}\Big\{ & U_\mu(x)U_\nu(x+\hat{\mu})U_\mu^\dagger(x+\hat{\nu})U_\nu^\dagger(x)+ \\ & +U_\nu(x)U_\mu^\dagger(x+\hat{\nu}-\hat{\mu})U_\nu^\dagger(x-\hat{\mu})U_\mu(x-\hat{\mu})+ \\ & +U_\mu^\dagger(x-\hat{\mu})U_\nu^\dagger(x-\hat{\nu}-\hat{\mu})U_\mu(x-\hat{\nu}-\hat{\mu})U_\nu(x-\hat{\nu})+ \\ & +U_\nu^\dagger(x-\hat{\nu})U_\mu(x-\hat{\nu})U_\nu(x-\hat{\nu}+\hat{\mu})U_\mu^\dagger(x) - \text{h.c.}\Big\}\,.\end{aligned}$$

# The N = 2 theories couples to fermions. Bulk phase structure: varying $N_{as}$.

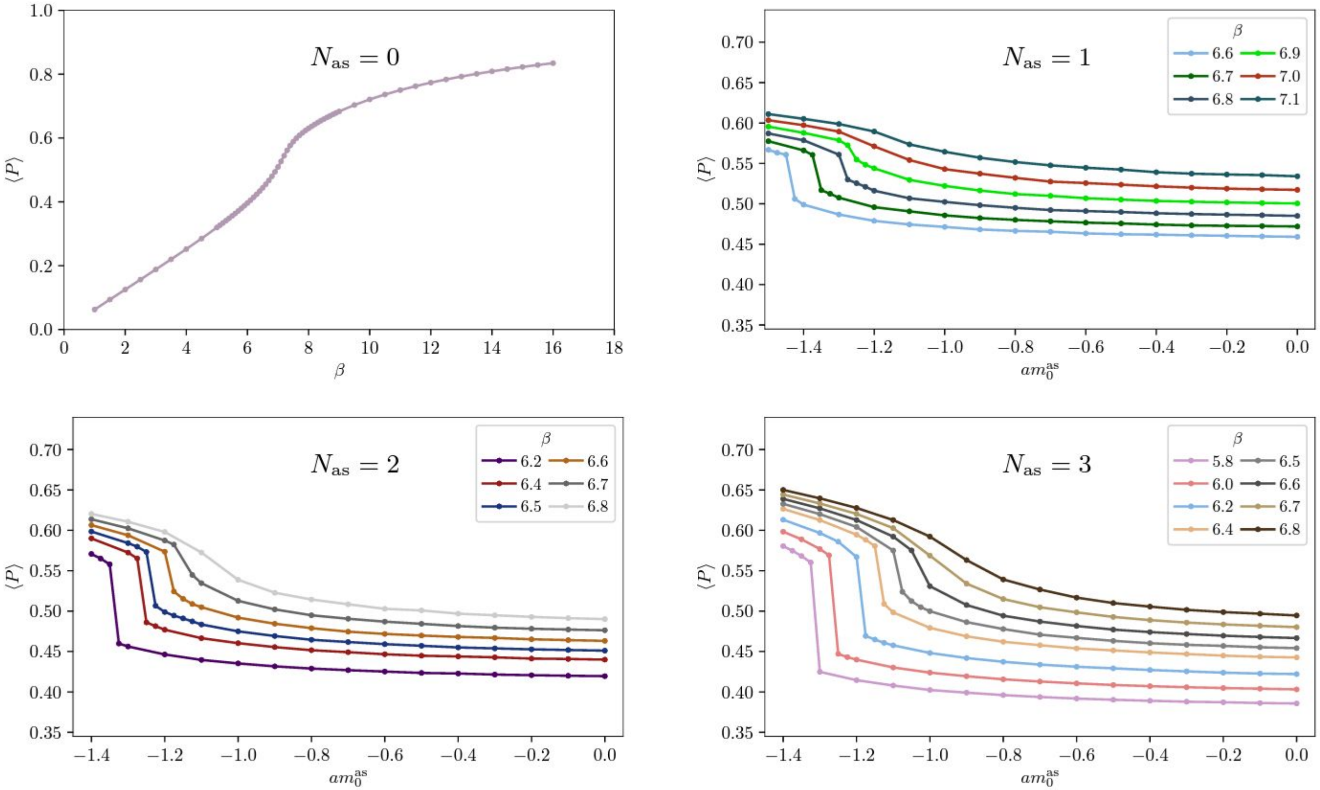


Fig D: Parameter scan of the Sp(4) theory with $N_{as}$ = 0,1,2,3, $N_f$ = 0 fermions.

# The N = 2 theories couples to fermions. Bulk phase structure: varying $N_{as}$. (2)

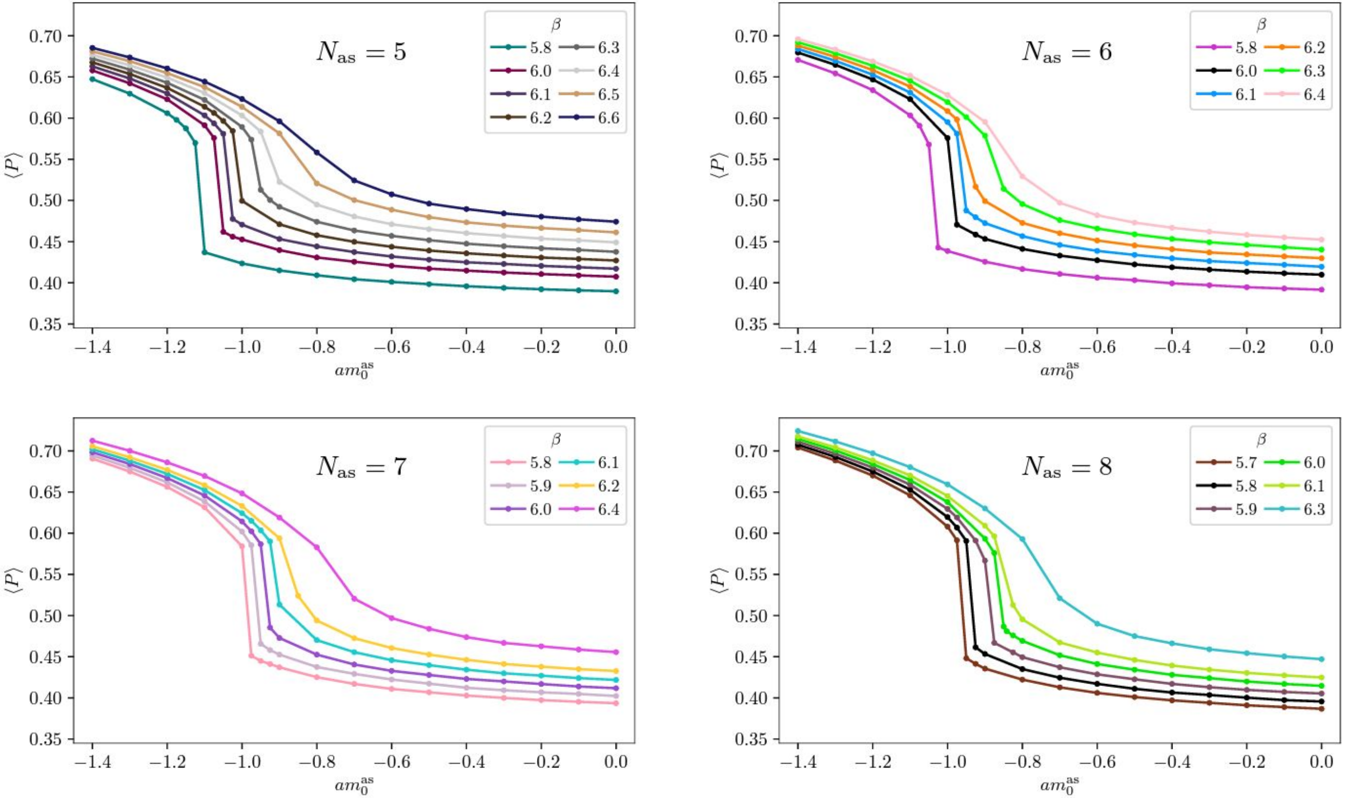


Fig E: Parameter scan of the Sp(4) theory with $N_{as}$ = 5,6,7,8, $N_f$ = 0 fermions.

# The N = 2 theories couples to fermions. Bulk phase structure. $N_{as}$ = 4, $N_f$ = 0 (2)

- We computed the *plaquette susceptibility*

$$\chi_P \equiv \frac{\tilde{V}}{a^4}\left(\langle P^2\rangle - (\langle P\rangle)^2\right)$$

  and compare the numerical results obtained with ensembles having two different volumes $\tilde{V} = (8a)^4$ $\tilde{V} = (16a)^4$ .

- When β is small, first order phase transition. When it's not, smooth crossover.

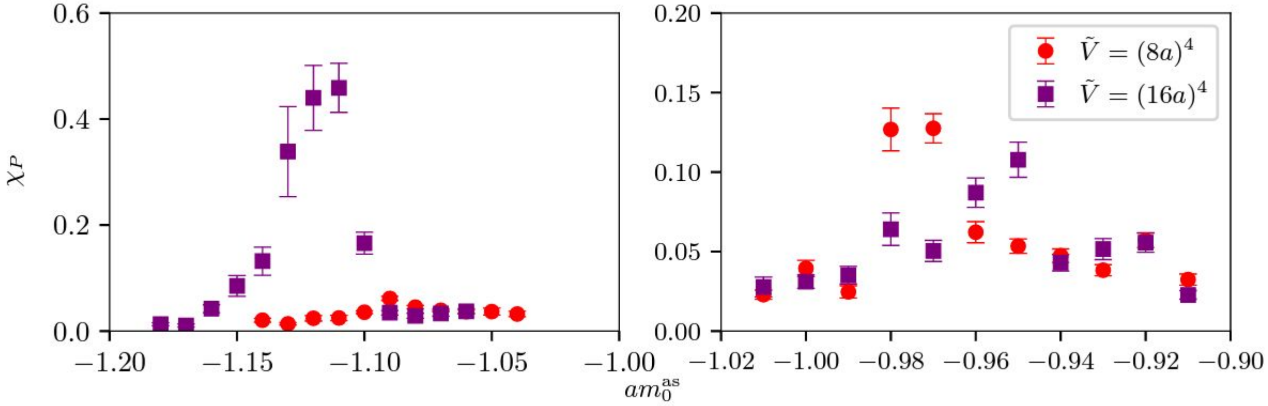


Fig F: Plaquette susceptibility of the Sp(4) theory with $N_{as}$ = 4, $N_f$ = 0 fermions, for β = 6.2 (left panel) and β = 6.5 (right panel).

# The conformal window

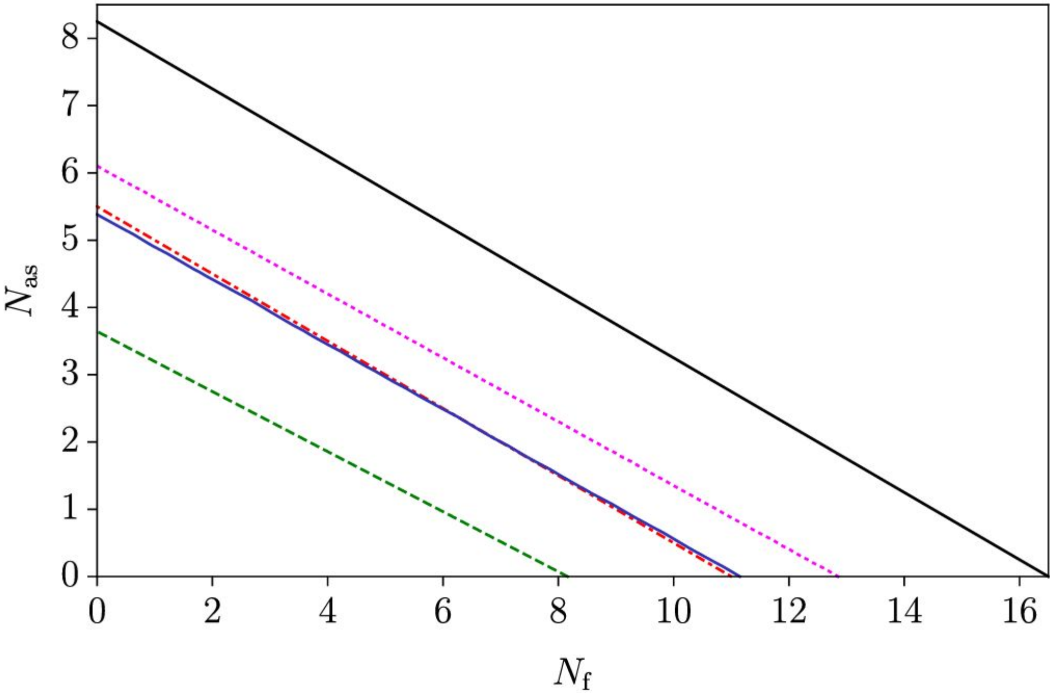


- The challenging question of identifying the lower end of the conformal window in these theories coupled to matter fields in various representations of the group requires the non-perturbative instruments of lattice field theory.

- This work, and the software we developed for it, set the stage needed to explore and quantify the extent of the conformal window in these theories.

Fig G: Estimates of the extent of the conformal window in Sp(4) theories coupled to Nf Dirac fermions transforming in the fundamental and Nas in the 2-index antisymmetric representation.